Appl Phys B (2012) 106:887–892
DOI 10.1007/s00340-011-4850-3

Applied Physics B
Lasers and Optics

Operation of femtosecond Kerr-lens mode-locked Cr:ZnSe lasers with different dispersion compensation methods

M.N. Cizmeciyan · H. Cankaya · A. Kurt · A. Sennaroglu

Received: 23 June 2011 / Revised version: 13 October 2011 / Published online: 14 January 2012

Abstract We employed various low-cost dispersion compensation methods to generate femtosecond pulses from a Kerr-lens mode-locked (KLM) Cr:ZnSe laser operating near 2400 nm. Prism pairs made of CaF_2 and MgF_2 and slabs of BK7 and YAG were tested. Pulses as short as 92 fs were obtained when a CaF_2 prism pair was used in the resonator with a 1% output coupler. With a 6% output coupler and CaF_2 prism pair, pulse energies as high as 1.8 nJ were obtained. The KLM operating point was further analyzed for different dispersion compensation scenarios by using the soliton area theorem to determine the nonlinear refractive index (n_2) of Cr:ZnSe. Results gave an n_2 value of $(1.2 \pm 0.2) \times 10^{-18}$ m^2/W in agreement with previous reports.

1 Introduction

Since its first demonstration in 1996 [1], Cr:ZnSe has emerged as a versatile solid-state source of tunable coherent radiation in the mid-infrared (mid-IR), covering the wavelength range 1880–3349 nm [2, 3]. Since the room-temperature luminescence quantum efficiency at low doping levels is close to unity, efficient continuous-wave (cw) operation can be readily obtained. Furthermore, the vibronically broadened emission band can be utilized to produce mode-locked pulses with picosecond [4] or femtosecond duration [5–7]. Mode-locked femtosecond Cr:ZnSe lasers have been used in mid-IR dual comb spectroscopy [8] and pumping of optical parametric oscillators operating at higher wavelengths [9]. In the direct measurement of the rovibrational absorption bands of molecules, frequency combs based on such mid-IR sources are more advantageous in comparison with their visible or near-infrared light counterparts which can only detect the overtone signals of the fundamental transitions with far lower excitation and emission efficiency [10]. Another potentially important application of ultrashort-pulse Cr:ZnSe lasers is in high harmonic generation. Here, studies show that in comparison with near-infrared sources, use of mid-IR sources has the potential of increasing the cut-off energy of the generated X-ray photons or attaining a particular cut-off energy with relatively lower excitation intensities [11, 12].

In previous studies, two main methods have been employed to generate femtosecond pulses from Cr:ZnSe lasers: semiconductor saturable absorber (SESAM) mode locking [5, 13], and Kerr-lens mode locking (KLM) [7]. In SESAM mode-locking experiments, pulses as short as 81 fs were obtained by using an InAs/GaSb-type multiple quantum-well saturable absorber. Here, dispersion compensation was achieved with a sapphire plate or chirped mirrors [5, 13]. In previous KLM experiments, either a YAG slab [6] or a MgF_2 prism pair [7] were used to obtain pulses as short as 95 fs. Irrespective of the mode locking method used, careful dispersion management of the resonator is very crucial in order to balance the nonlinearities stemming from the Kerr medium and/or the saturable absorber. To manage the group delay dispersion (GDD), various types of optical elements, including prism pairs, dispersion compensating mirrors (DCM), Gires–Tournois interferometer (GTI) mirrors, and slabs, can be used. The ideal choice of the dispersion compensator depends on several factors, including the amount of negative

M.N. Cizmeciyan · H. Cankaya · A. Sennaroglu (✉)
Laser Research Laboratory, Department of Physics,
Koç University, Rumelifeneri, Sariyer, Istanbul 34450, Turkey
e-mail: asennar@ku.edu.tr

A. Kurt
Teknofil, Inc., Zekeriyakoy, Istanbul 34450, Turkey

GDD that can be produced, the level of residual third-order dispersion, and the insertion loss of the compensator. Commercial DCMs and GTI mirrors are available for femtosecond lasers in the visible and near-infrared light. However, at present, such dispersion compensators are not readily commercially available at mid-IR wavelengths. If slabs or prism pairs are used as an alternative, the emission band of the laser should coincide with the transparency window of the materials that will be used as slabs or prisms. These considerations show that it is important to develop cost-effective dispersion management methods for lasers that operate in the mid-IR range.

In this work, we evaluated the performance of a femtosecond Kerr-lens mode-locked (KLM) Cr:ZnSe laser operated near 2400 nm with various low-cost dispersion compensation methods. Prism pairs made of CaF_2 and MgF_2, and slabs of BK7 and YAG were investigated. Pulses as short as 92 fs were obtained when a CaF_2 prism pair was used in the resonator for dispersion compensation. With a 6% output coupler and CaF_2 prism pair, pulse energies as high as 1.81 nJ were obtained. The KLM operating point was further analyzed for different combinations of dispersion, output coupling, and pulse energy to determine the nonlinear refractive index (n_2) of Cr:ZnSe. Results gave an n_2 value of $(1.2 \pm 0.2) \times 10^{-18}$ m^2/W in agreement with previous reports. Although MgF_2 prism pairs and YAG slabs were used in previous mode-locking studies [6, 7], we also included our results taken with these compensation schemes for the sake of completeness and also to collect sufficient data for the determination of the nonlinear refractive index of the Cr:ZnSe medium.

2 Experimental

As can be seen from the schematic of the experimental setup shown in Fig. 1, the Cr:ZnSe laser was configured as a standard, astigmatically compensated x-resonator with two curved high reflectors (M1 and M2, $R = 10$ cm) around the 2.4-mm-long, single-crystal Cr:ZnSe gain medium, a flat-end high reflector (HR) and a flat-output coupler (OC). Two different output couplers with 1 and 6% transmission at 2400 nm were used in the experiments. The high reflector and the output coupler arm lengths were 65 and 84 cm, respectively, giving an estimated beam waist of 34.9 μm near the center of the cavity stability range. The total small-signal absorption of the Cr:ZnSe gain medium at 1800 nm was 94%. To remove the unused pump power, the crystal was surrounded with indium foil and held inside a copper holder whose temperature was maintained at 21°C by water cooling. The Cr:ZnSe laser was longitudinally pumped with a continuous-wave (cw) Tm-fiber pump laser operating at 1800 nm. The pump beam was focused inside the gain

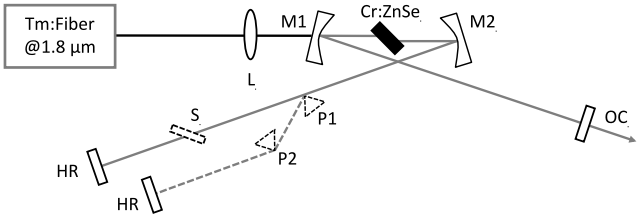

Fig. 1 Experimental setup of the Kerr-lens mode-locked Cr:ZnSe laser containing a slab (S) or a prism pair (P1 and P2) for dispersion compensation

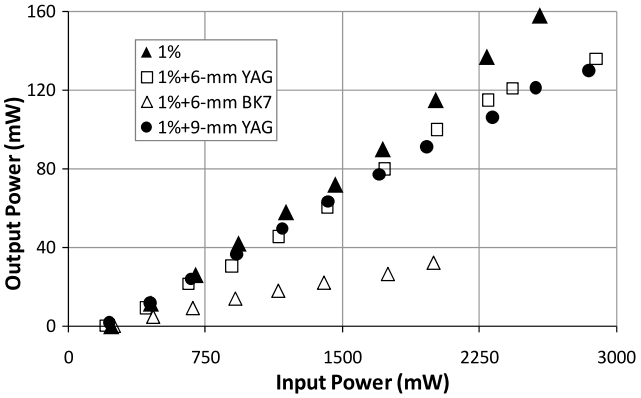

Fig. 2 Continuous-wave power efficiency curves of the Cr:ZnSe laser containing 6-mm BK7, 6-mm YAG, and 9-mm YAG slabs. The transmission of the output coupler is 1%

medium with a converging lens of focal length 10 cm (L in Fig. 1). During KLM operation, either a prism pair (P1 and P2) or a slab (S) was used for dispersion compensation. In the initial phase of the experiments, the cw power performance of the resonator was evaluated in the absence of dispersion compensation elements. As can be seen from Fig. 2, output power as high as 158 mW was obtained with the 1% output coupler when the input pump power was 2.58 W. The corresponding slope efficiency (η_s) was measured to be 6.7%. In the case of the 6% output coupler, the slope efficiency was 14.5% and a maximum of 370 mW was obtained with 2.82 W of pump power (see Fig. 3). In the experiments, soft-aperture Kerr-lens mode locking was employed to initiate the pulse train by optimizing the focusing inside the gain medium and by translating the output coupler. During mode-locked operation, dispersion compensation elements (prism pair or slab) were placed at Brewster incidence in the high reflector arm of the laser. Figures 2, 3, and 4 also show the power performance of the laser with these elements. The cavity was further purged with N_2 gas to maintain a relative humidity level around 30% and to minimize instabilities due to water absorption. The spectral and temporal characteristics of the mode-locked pulses were measured with a mid-IR scanning spectrometer and an intensity autocorrelator. Two-photon absorption in a Ge detector was utilized to measure the intensity autocorrelation of the pulses.

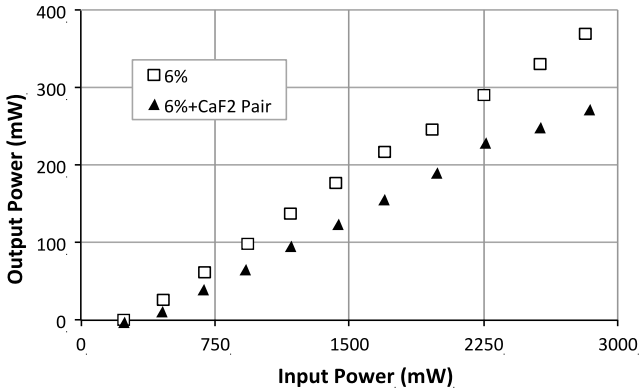

Fig. 3 Continuous-wave power efficiency curves of the Cr:ZnSe laser with a CaF_2 prism pair and a 6% output coupler

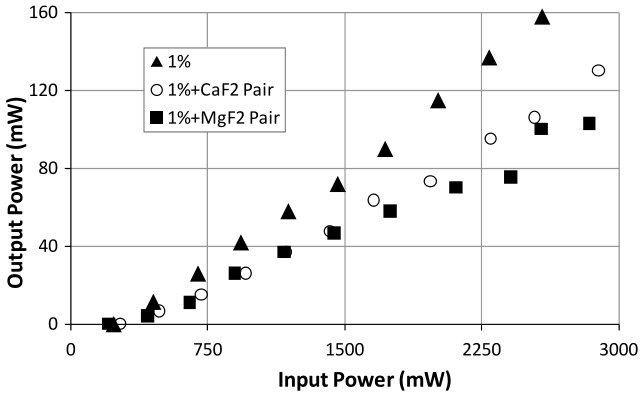

Fig. 4 Continuous-wave efficiency curves of the Cr:ZnSe laser with MgF_2 and CaF_2 prism pairs. The transmission of the output coupler is 1%

3 Results and Analysis

The power performance of the mode-locked Cr:ZnSe laser was first evaluated with different intracavity dispersion compensation slabs (S in Fig. 1), and prism pairs (P1 and P2 in Fig. 1). Table 1 lists the estimated insertion loss of the compensation element, net group delay dispersion (GDD) of the resonator containing the compensation element, mode-locked pulse-width, repetition rate, and time-bandwidth product for each configuration. The loss introduced by each dispersion compensation element was estimated in two steps. First, the round-trip loss L_C of the resonator was estimated by comparing the slope efficiencies obtained with two different output couplers in the free-running regime and by using the equation

$$\eta_1 = \frac{\frac{T_1}{T_1+L_C}}{\frac{T_2}{T_2+L_C}}. \tag{1}$$

Here, T_1 and T_2 stand for the power transmission of the two different output couplers and η_1 is the ratio of the slope efficiencies measured with these two output couplers. In our case, $T_1 = 1\%$ and $T_2 = 6\%$. By using the measured slope efficiencies and (1), L_C was determined to be 1.79%. In the next step, we compared the slope efficiency of the original free-running laser (operated with the output coupler having transmission of T_1) with that of the resonator containing the same output coupler and also the dispersion compensation element. The round-trip loss of the compensator was assumed to be L_{DC}. From the ratio η_2 of the measured slope efficiencies, L_{DC} was estimated by using the equation

$$\eta_2 = \frac{\frac{T_1}{T_1+L_C}}{\frac{T_1}{T_1+L_C+L_{DC}}}. \tag{2}$$

As can be seen from Table 1, the worst cw and mode-locked performance was obtained when the 6-mm-long BK-7 slab was used for dispersion compensation. In this case, the estimated loss introduced by the slab was 16.3% and, as can be seen from Fig. 2, only 32 mW of cw output power could be obtained with 2 W of pump power (a corresponding slope efficiency = 1.72%). Excess loss limited the mode-locked pulse energy to 0.22 nJ and the shortest obtained pulse-width was 385 fs.

The cw performance of the laser was dramatically improved by using YAG slabs which have low absorption loss in the operating wavelength range of the Cr:ZnSe laser. For example, the estimated insertion loss of the 6- and 9-mm YAG slabs was 1.4 and 1.9%, respectively. In the case of the 6-mm-long YAG substrate, the net GDD of the cavity (-1092 fs^2) was not sufficient to balance the Kerr nonlinearities and double pulsing was routinely observed in the autocorrelation trace. Addition of an extra 3-mm-long YAG plate nearly doubled the net GDD to -2164 fs^2. In this case, double pulsing disappeared and 41 mW of average output power was obtained, corresponding to 0.45 nJ of pulse energy. For the mode-locked resonator containing 9-mm-long YAG slab, the measured spectrum and autocorrelation of the pulses are shown in Fig. 5(a) and (b), respectively. By assuming a sech^2 pulse profile, the pulse-width (FWHM) was determined to be 121 fs. The spectral bandwidth was 61 nm, giving a time-bandwidth product of 0.374.

Although a single-crystal YAG slab can be used with very low insertion loss to compensate for dispersion around 2400 nm, the fixed length of the substrate prevents continuous adjustment of the total GDD. This can be obviated by using prism pairs where GDD can be varied by changing the prism separation and/or prism material insertion. In our experiments, we tested the performance of two types of prism pairs (MgF_2 and CaF_2) which have high transmission around 2400 nm. In each case, the prisms were inserted at Brewster incidence on the high reflector arm of the cavity. They were further mounted on translation stages to control the material insertion. Figure 4 shows the cw power performance of each prism pair taken with the 1% transmitting

Table 1 Output coupler transmission (T), slope efficiency (η_s), estimated insertion loss (L_{DC}), pulse-width (τ_p), spectral width ($\Delta\lambda$), central wavelength (λ_p), time-bandwidth product ($\tau_p \cdot \Delta\nu$), calculated group delay dispersion (GDD), third-order dispersion (TOD), average output power (P_{av}), repetition rate (f_{rep}), and output pulse energy (W_{out}) of the KLM Cr:ZnSe laser operated with different dispersion compensation schemes. GDD and TOD values were estimated by using the Sellmeier data [15] and dispersion equations [16]

Dispersion element	T (%)	η_s (%)	L_{DC} (%)	τ_p (fs)	$\Delta\lambda$ (nm)	λ_p (nm)	$\tau_p \cdot \Delta\nu$	GDD (fs^2)	TOD (fs^3)	Pav (mW)	f_{rep} (MHz)	W_{out} (nJ)
6-mm YAG	1	5.4	0.7	116	69	2450	0.404	−1092	14149	31	190	0.16
9-mm YAG	1	5.0	1.0	121	61	2427	0.374	−2164	20068	41	91	0.45
6-mm BK7	1	1.7	8.3	385	27	2361	0.556	−1758	16738	22	91	0.22
MgF_2 pair	1	3.7	2.3	95	69	2421	0.335	−1606	18029	40	100	0.40
CaF_2 pair	1	5.0	1.0	92	76	2459	0.348	−1767	20550	31	95	0.33
CaF_2 pair	6	11.2	2.3	121	63	2451	0.379	−1773	20343	165	95	1.81

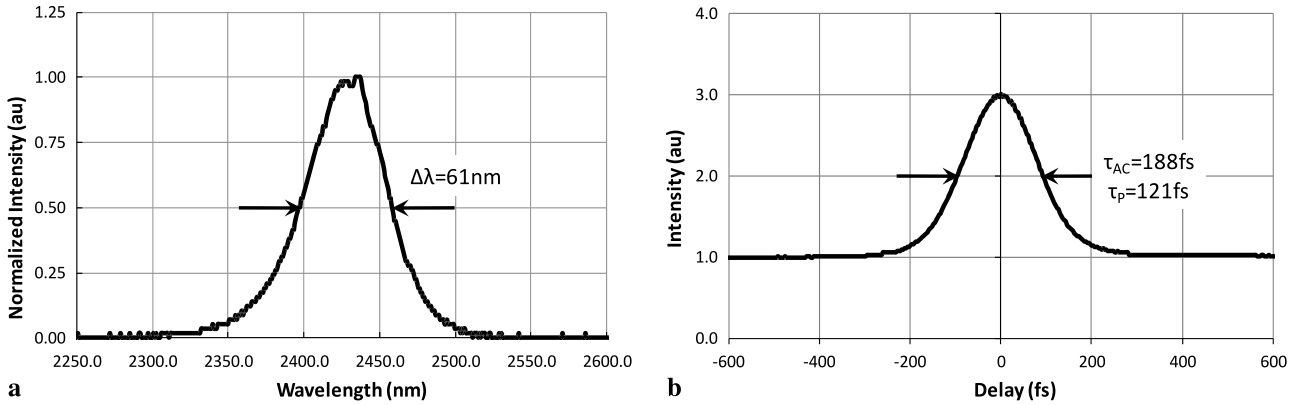

Fig. 5 (**a**) Measured spectrum and (**b**) autocorrelation of the pulses generated from the KLM Cr:ZnSe laser containing a 1% output coupler and a 9-mm YAG slab

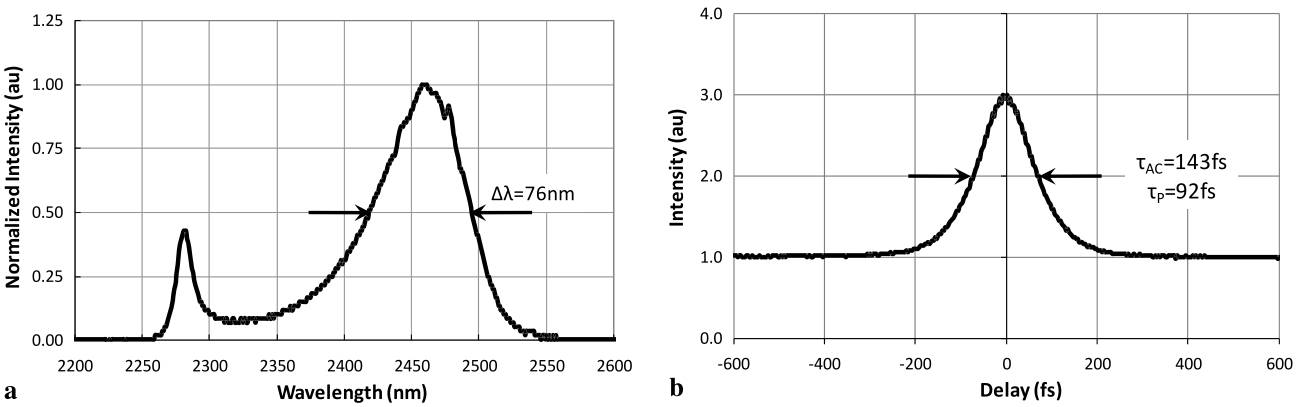

Fig. 6 (**a**) Measured spectrum and (**b**) autocorrelation of the pulses generated from the KLM Cr:ZnSe laser containing a 1% output coupler and a CaF_2 prism pair

output coupler. As can be seen from Table 1, the insertion loss of the CaF_2 prism pair (2.0%) was lower than that of the MgF_2 prism pair (4.6%) due to the better surface quality of the former. In particular, the resonator containing the CaF_2 prism pair and the 1% output coupler produced 73 mW of output power with 1.97 W of pump power, which was 6 mW higher than that obtained with the MgF_2 prism pair. For both cases, the net GDD of the cavity was in the range of $-(1600–1800)$ fs^2, resulting in the generation of sub-100-fs pulses. With the CaF_2 prism pair, slightly shorter pulses with duration of 92 fs were generated. The pulse energy and time-bandwidth product were 0.33 nJ and 0.348, respectively. For

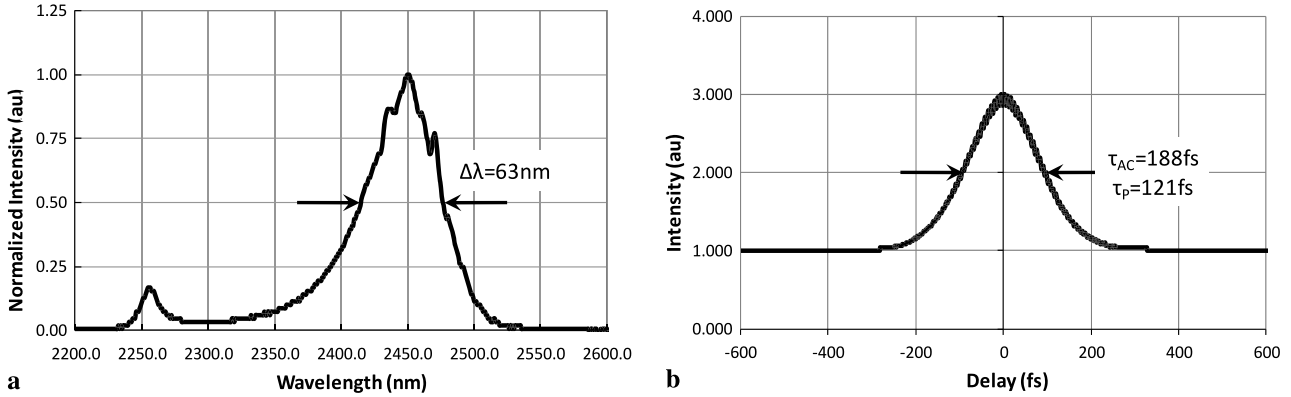

Fig. 7 (**a**) Measured spectrum and (**b**) autocorrelation of the pulses generated from the KLM Cr:ZnSe laser containing a 6% output coupler and a CaF_2 prism pair

the mode-locked resonator containing the CaF_2 prism pair, the measured spectrum and autocorrelation of the pulses are shown in Fig. 6(a) and (b).

Finally, in order to extract higher pulse energies from the laser, the 1% output coupler was replaced with a 6% output coupler while keeping the CaF_2 prism pair in the high reflector arm of the laser. As can be seen from Table 1, this gave as high as 165 mW of average output power during mode-locked operation, corresponding to 1.81 nJ of pulse energy at the pulse repetition frequency of 95 MHz. As can be seen from the autocorrelation and spectrum measurements displayed in Fig. 7(a) and (b), the temporal and spectral widths of the pulses were 121 fs and 63 nm, giving a time-bandwidth product of 0.379. In this case, no double pulsing was observed with a fast detector that monitored the pulse train in the nanosecond timescale or with the autocorrelator.

The KLM operating point of each configuration can be analyzed by using the soliton area theorem that relates the output pulse-width to the pulse energy, GDD, and nonlinear refractive index [14]. In particular, we can determine the nonlinear refractive index n_2 from the experimentally measured parameters of the mode-locked laser by using the well-known equation

$$\tau = \frac{4|D|}{W\delta}. \tag{3}$$

Here, τ is the pulse-width divided by 1.76, W is the intracavity pulse energy, D is the net GDD of the cavity, and δ is the nonlinear coefficient given by

$$\delta = \frac{2\pi}{\lambda} n_2 \frac{2L_C}{A_{\text{eff}}}. \tag{4}$$

In (4), λ is the center wavelength of the spectrum, L_C is the single-pass length of the gain medium, and A_{eff} is the effective area of the laser beam inside the gain medium given by

$$A_{\text{eff}} = n_0 \pi \omega_{\text{rms}}^2/2. \tag{5}$$

Table 2 The nonlinear refractive index (n_2) values determined by using the soliton area theorem for the different mode-locking configurations tested in the experiments

Dispersion element	OC (%)	n_2 (m^2/W)
6-mm YAG	1	1.49×10^{-18}
9-mm YAG	1	1.01×10^{-18}
6-mm BK7	1	5.12×10^{-19}
MgF_2 pair	1	1.07×10^{-18}
CaF_2 pair	1	1.52×10^{-18}
CaF_2 pair	6	1.55×10^{-18}
Average		1.2×10^{-18}

In (5), n_0 is the linear refractive index and ω_{rms} is the root-mean-squared spot-size of the laser beam. In the calculation of ω_{rms}, we employed the standard ABCD analysis to first determine the beam waist (ω_0) inside the gain medium. Here, it was assumed that the cavity configuration remains near the center of the stability region during KLM operation and ω_{rms} was calculated by using the equation

$$\omega_{\text{rms}} = \sqrt{\frac{1}{L_C}\int_0^{L_C} \omega_0^2 \left(1 + \left(\frac{z - z_f}{z_0}\right)^2\right) dz}. \tag{6}$$

In (6), z_f is the location of the laser beam waist within the crystal and z_0 is the Rayleigh range ($z_0 = n_0 \pi \omega_0^2/\lambda$). The parameters ω_0 and ω_{rms} were determined to be 34.9 and 35.5 μm, respectively. By using this procedure, the nonlinear refractive index n_2 was determined for each of the six KLM configurations tested in the experiments and the results are tabulated in Table 2. The nonlinear refractive index n_2 came to $(1.2 \pm 0.2) \times 10^{-18}$ m^2/W which is close to the previously reported value of 1.7×10^{-18} m^2/W [13].

4 Conclusions

We have utilized four different cost-effective and practical dispersion compensation methods for Cr:ZnSe lasers operated in the Kerr-lens mode-locked regime. Our results show that, in the case of BK7, although material dispersion has the correct sign to compensate for Kerr nonlinearities, the excessive material absorption leads to poor power and mode-locked performance. The highest pulse energy was obtained with a 6% output coupler and a CaF_2 prism pair, where as high as 1.81 nJ was obtained with 2 W of pump power. When a 1% output coupler was used with the CaF_2 prism pair, higher intracavity energy led to the generation of the shortest pulses (duration of 92 fs FWHM) in the experiments. Overall, YAG slabs could be used with lower insertion loss in comparison with prism pairs. On the other hand, the prism pair allowed for continuous adjustment of the cavity dispersion. Finally, by using the soliton area theorem, we estimated the nonlinear refractive index (n_2) of ZnSe as $(1.2 \pm 0.2) \times 10^{-18}$ m^2/W, which comes close to the previously reported value of 1.7×10^{-18} m^2/W.

Acknowledgements This project was supported by the Scientific and Technological Research Council of Turkey (Tubitak, Project No. 108T028). We would also like to thank Refik Kortan for donating some of the equipment used in the experiments.

References

1. L.D. DeLoach, R.H. Page, G.D. Wilke, S.A. Payne, W.F. Krupke, IEEE J. Quantum Electron. **32**, 885 (1996)
2. U. Demirbas, A. Sennaroglu, Opt. Lett. **31**, 2293 (2006)
3. E. Sorokin, I.T. Sorokina, M.S. Mirov, V.V. Fedorov, I.S. Moskalev, S.B. Mirov, Ultrabroad continuous-wave tuning of ceramic Cr:ZnSe and Cr:ZnS lasers. Paper AMC2 at Advanced Solid-State Photonics, San Diego, CA, February 2010
4. T.J. Carrig, G.J. Wagner, A. Sennaroglu, J.Y. Jeong, C.R. Pollock, Opt. Lett. **25**, 168 (2000)
5. I.T. Sorokina, E. Sorokin, T. Carrig, Femtosecond pulse generation from a SESAM mode-locked Cr:ZnSe laser. Paper CMQ2 at Conference on Lasers and Electro-Optics (CLEO), Long Beach, CA, May 2006
6. E. Sorokin, I.T. Sorokina, Ultrashort-pulsed Kerr-lens mode-locked Cr:ZnSe laser. Paper CF1.3 WED at CLEO/Europe, Munich, June 2009
7. M.N. Cizmeciyan, H. Cankaya, A. Kurt, A. Sennaroglu, Opt. Lett. **34**, 3056 (2009)
8. B. Bernhardt, E. Sorokin, P. Jacquet, R. Thon, T. Becker, I.T. Sorokina, N. Picque, T.W. Hansch, Appl. Phys. B, Lasers Opt. **100**, 3 (2010)
9. K. Vodopyanov, E. Sorokin, P. Schunemann, I. Sorokina, 4.4–5.4 μm frequency comb from a subharmonic OP-GaAs OPO pumped by a femtosecond Cr:ZnSe laser. Paper AME2 at Advanced Solid-State Photonics, Istanbul, February 2011
10. F. Adler, K.C. Cossel, M.J. Thorpe, I. Hartl, M.E. Fermann, J. Ye, Opt. Lett. **34**, 1330 (2009)
11. A. Gordon, F.X. Kartner, Opt. Express **13**, 2941 (2005)
12. H. Xiong, H. Xu, Y. Fu, J. Yao, B. Zeng, W. Chu, Y. Cheng, Z. Xu, E.J. Takahashi, K. Midorikawa, X. Liu, J. Chen, Opt. Lett. **34**, 1747 (2009)
13. I.T. Sorokina, in *Broadband Mid-Infrared Solid-State Lasers in Mid-Infrared Coherent Sources and Applications*, ed. by M. Ebrahim-Zadeh, I.T. Sorokina (Springer, Berlin, 2007)
14. H.A. Haus, IEEE J. Sel. Top. Quantum Electron. **6**, 1173 (2000)
15. M. Bass, *Handbook of Optics* (McGraw-Hill, New York, 1994)
16. R.L. Fork, C.H.B. Cruz, P.C. Becker, C.V. Shank, Opt. Lett. **12**, 483 (1987)